Desalination and Water Treatment
www.deswater.com

doi: 10.1080/19443994.2013.767752

51 (2013) 5746–5754
August

Taylor & Francis
Taylor & Francis Group

Hydrochemical evaluation of sodium chloride and sodium sulphate groundwater in the Kaboudar Ahang, Hamedan, western Iran

Mohsen Jalali

Department of Soil Science, College of Agriculture, Bu-Ali Sina University, Hamadan, Iran
Tel. +98 811 4227012; Fax: +98 811 4227090; email: Jalali@basu.ac.ir

Received 12 September 2012; Accepted 15 December 2012

ABSTRACT

Hydrogeochemical investigation of groundwater in the Kaboudar Ahang, Hamedan, western Iran was carried out to assess chemical composition of groundwater having complex contamination sources. The chemical compositions of the groundwater are dominated by Na^+, Cl^- and SO_4^{2-}. The predominant water type of groundwater samples are the NaCl (59%) and NaSO4 (38%) facies. Both Na^+ and $Cl^- + SO_4^{2-}$ account for 56 and 61% of the total cations and anions. Contamination of groundwater appeared to be affected by the solubility of mineral phases and discharge of sewage effluent, and agricultural activities. Anthropogenic inputs into the groundwater mainly include Na^+, Cl^- and SO_4^{2-} according to chemical compositions of sewage effluent. Continuous disposal of sewage effluent from power plant (which contains appreciable amounts of Na^+ ions) through irrigation in closed systems poses a serious threat of soil and groundwater sodification.

Keywords: Geochemistry; Groundwater; Contamination; Inverse modelling; Sewage effluent

1. Introduction

Water shortages have become an increasingly serious problem in Iran, especially in the arid and semi-arid regions of the western Iran [1]. Groundwater has become the major source of water supply for domestic, industrial and agricultural sectors of many countries. The monitoring of water quality is one of the important tools for sustainable development and provides important information for water management. Measuring and identifying the mass loading of pollutant to groundwater from specific agricultural and industrial systems seems to be useful aids in controlling contaminations in groundwater.

Numerous publications have reported that urban development and agricultural activities directly or indirectly affect groundwater quality [2–4]. Agricultural contamination of groundwater usually results from routine applications of agrochemicals on cropped fields and a process that accumulates the nutrients in groundwater. Pesticides, herbicides, fungicide and other chemicals also affect groundwater quality. Groundwater nitrate (NO_3^-) and chloride (Cl^-) contamination can result from the overapplication of manure and fertilizer [5,6]. In Iran, agricultural land may be considered the main source of NO_3^- where intensification in the last thirty years has increased NO_3^- leaching from soils into both surface and groundwater [4], but urbanization and industrial activities may also responsible for NO_3^- in groundwater.

The evaluation and management of groundwater resources require an understanding of hydrogeological and hydrochemical properties of the aquifer [7]. In Kaboudar Ahang, a part of Hamedan province, western Iran, the aquifers are of major importance as they are the main source of water supply. Groundwater and soils in this area are vulnerable to contamination and once contaminated their rehabilitation is difficult and time-consuming project. Due to the various contaminant sources, complicated chemical processes control the groundwater quality. On the basis of physical and chemical properties of soils, some soils in the studied area are classified as saline-sodic and saline [8]. Thus, hydrogeochemical investigation was carried out in Kaboudar Ahang area to identify groundwater contamination processes.

2. Study area

The study area lies between longitudes 48° 32′ and 48° 55′ E and latitudes 35° 3′ and 35° 25′ N, with a mean altitude of 1,746 m.a.s.l (Fig. 1). The climate of the study area is considered to be semi-arid, the annual average precipitation being approximately 300 mm, of which about 37% occurs during winter. The mean air monthly temperature is highest during August (23.45°C) and lowest during January (−1.91°C) with an annual average of 10.88°C. Groundwater has been used for various purposes such as drinking, agricultural, domestic and industrial needs. Within the last 30 years, the rapid urbanization and industrialization in addition to the overexploitation and utilization of groundwater have resulted in lowering groundwater level and groundwater contamination in this area.

The Sanandaj–Sirjan zone, that extends over 1,300 km, is a major structural NW–SE trend in south-western Iran. The Hamedan area, a part of Sanandaj–Sirjan, is characterized by the predominance of metamorphic rocks of both sedimentary and magmatic origins [9] and the presence of the Alvand huge granitoid complex. The methamorphic rocks constitute an assemblage of high to low methamorphic grade rocks from sedimentary sequences that have been affected by a more- or less-developed tectonometamorphic events [10]. Basement rocks and minerals in the studied area consist of granites, schist, plagioclase, dolomite and limestone.

3. Materials and methods

3.1. Sample collection and analysis

Forty-two groundwater samples were selected based on the preliminary field survey from Kaboudar Ahang in the Hamedan Province, August 2005 (Fig. 1). Samples were analysed in the laboratory for the major ions employing standard methods. The determinations were made within 48 h of collection. The pH and electrical conductivity (EC) were measured using pH and electrical conductivity meters. Calcium (Ca^{2+}) and magnesium (Mg^{2+}) were determined titrimetrically using standard EDTA. Chloride was determined by standard $AgNO_3$ titration. Carbonate (CO_3^{2-}) and bicarbonate (HCO_3^-) were determined by titration with HCl. Sodium (Na^+) and potassium (K^+) ions were measured by flame photometry, sulphate ions (SO_4^{2-}) by spectrophotometric turbidimetry and NO_3^- ions by colorimetry with a UV–visible spectrophotometer [11]. Silicon (Si) and aluminium (Al) ions were measured by ICP and dissolved P was

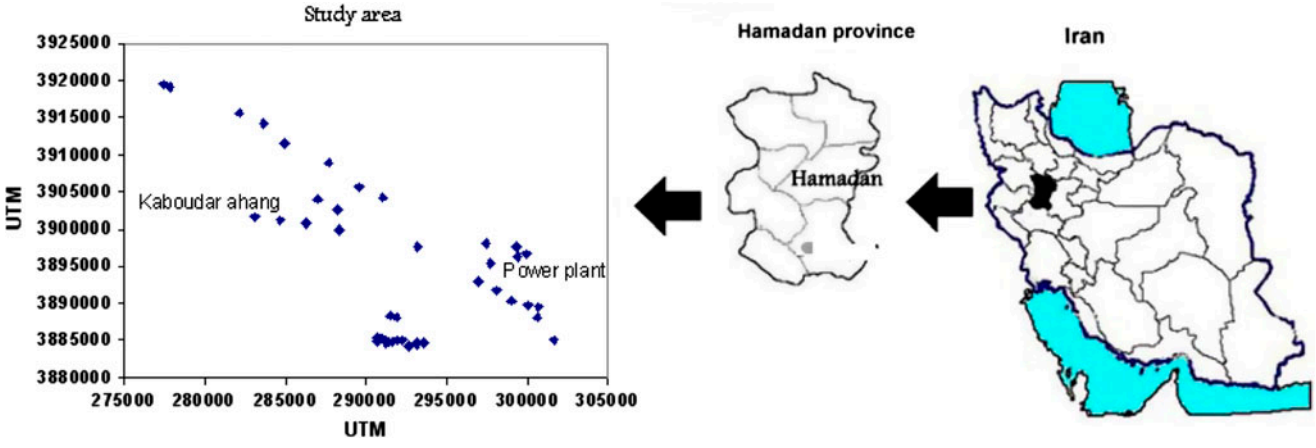

Fig. 1. Study area showing location of wells sampled for groundwater analysis.

measured by the phosphomolybdo-blue reduction with ascorbic acid method [12].

In order to evaluate saturation indices (SI) (the ratio of ion activity product to solubility product) and mass transfers in the water–rock system, the geochemical code PHREEQC [13] was used. The corresponding samples were chosen taking into account the geographical position of the sampling point and observed hydrochemical trends (Na^+ increase along flowpath). The analytical precision for the measurements of ions was determined by the ionic balances, calculated as $100 \times (\text{cations} - \text{anions})/(\text{cations} + \text{anions})$, which is generally within ± 5%. The statistical software package MINITAB (version 13.1, Minitab Inc.) was employed for the calculations.

4. Results and discussion

4.1. Summary statistics

Table 1 shows the chemical compositions of groundwater, together with electrical conductivity and pH. Cl^- is the dominant anion and its concentrations in water samples range between 53 and 235 mg l^{-1}, whereas the concentrations of Na^+ vary from 67 to 258 mg l^{-1}. The concentrations of Ca^{2+} range between 18 and 76 mg l^{-1}, the Mg^{2+} concentrations range between 9 and 42 mg l^{-1} and the SO_4^{2-} concentrations range from 38 to 403 mg l^{-1}. The pH values of groundwater are within the range of 7.3–8.4 (averaging 7.8). The PO_4^{2-} concentration range in groundwater was 0.02–0.18 mg l^{-1}, with an average value of 0.11 mg l^{-1}. Concentrations of SiO_2 ranged between 18 and 38 mg l^{-1} and concentrations of Al ranged between 0.2 and 0.6 mg l^{-1}.

Nearly 19% of water samples were oversaturated with respect to calcite and dolomite (Table 2). Water samples were undersaturated with respect to sulphur-bearing minerals (gypsum and anhydrite). All other mineral phases which could control NaCl in the aquifer are largely undersaturated. Water samples were undersaturated with respect to hydroxyapatite. Water samples were saturated with respect to quartz and undersaturated with respect to amorphous silica. The dissolution of silicate minerals is generally a very slow process that does not produce significant variations in the water chemistry [14]. Illite and vermiculite were present in the soils [15] and could have served as a source of Si in groundwater. Water samples were undersaturated with respect to amorphous aluminium and alunite and saturated with respect to gibbsite and albite (95%).

Groundwater are dominated by Na^+, Cl^- and SO_4^{2-}, which account for about 56% and 62% of total cations and anions, respectively. Calcium and Mg^{2+} are generally about 23 and 21%, respectively. The HCO_3^- anion is less than 21% of the total anions. Based on dominant cations and anions, two main groundwater groups have been identified: NaCl and $NaSO_4$.

The NaCl and $NaSO_4$ each represent 59 and 38% of the total number of water samples analysed. The NaCl-type water is dominated in the most part of studied area.

4.2. Ionic relations

Fig. 2(a) shows the value of Cl^- as a function of Na^+ in the groundwater samples and there is significant correlation ($r = 0.57$) (Table 3) between them. A Na^+/Cl^- molar ratio approximately equal to one is usually attributed to halite dissolution, whereas a ratio greater than one is typically interpreted as reflecting Na^+ released from silicate weathering reactions. Almost all of the groundwater samples have the equivalent ratios of Na^+/Cl^- larger than one, indicating excess of Na^+ over Cl^-. There is a strong positive correlation ($r = 0.80$) between Na^+ and SO_4^{2-} Fig. 2b), indicating that the excess of Na^+ in these samples mostly result from dissolution of sodium sulphate minerals.

The cation exchange between Ca^{2+} or Mg^{2+} and Na^+ may also explain the excess Na^+ concentration [16,17]. Calcium and Mg^{2+} can exchange Na^+ sorbed on the exchangeable sites of the clay minerals, resulting the decrease of Ca^{2+} and Mg^{2+} and increase of Na^+ in groundwater.

There are other sources of Na^+ and Cl^- in the groundwater such as wastewater. Usually wastewater is enriched in Na^+ relative to Cl^- [18]. A reduction in the Na^+ to Cl^- ratio with time and/or distance as a result of the exchange of Na^+ with other cations has been observed in studies of deicing salts [18,19] and wastewater [18]. Therefore, even if halite is the dominant source of Na^+ and Cl^- in the groundwater, the molar ratio will vary spatially and temporally as a result of cation exchange [20]. This ratio should also decrease due to the cation exchange of Na^+ as water moves through the aquifer, which would explain Cl^- enrichment in most water samples.

4.3. Carbonate dissolution by sulphuric acid

Dissolution of carbonate minerals may take place due to the attack of H_2CO_3 and H_2SO_4 [21]. One possible source of SO_4^{2-} may be from dissolution of sulphate evaporate. Fig. 3 shows the variations of the $Ca^{2+} + Mg^{2+}/HCO_3^-$ with SO_4^{2-}/HCO_3^- equivalent ratios for the samples. For those waters that have

Table 1
Summary statistics of chemical compositions of major ions ($mg\,l^{-1}$) in the groundwater of Kaboudar Ahang area

Well No.	Variable													
	EC μS cm^{-1}	pH	Ca^{2+}	Mg^{2+}	Na^{+}	K^{+}	HCO_3^-	CO_3^{2-}	Cl^-	SO_4^{2-}	NO_3^-	PO_4^{3-}	SiO_2	Al
1	787	7.39	48	17	87	0.22	92	33	80	122	12	0.12	18	0.3
2	706	7.62	34	23	81	0.19	67	30	111	91	10	0.09	25	0.3
3	809	7.74	28	31	76	0.20	92	30	89	115	11	0.06	25	0.3
4	791	7.41	44	18	76	0.21	140	30	80	72	16	0.09	25	0.2
5	821	7.48	40	25	89	0.21	165	36	98	53	10	0.12	24	0.3
6	860	7.65	50	34	78	0.25	110	15	115	142	22	0.06	26	0.6
7	890	7.30	64	26	81	0.24	122	30	137	82	20	0.09	27	0.5
8	880	7.42	54	36	67	0.25	122	15	129	101	20	0.12	27	0.5
9	930	7.59	46	31	87	0.23	153	30	124	83	17	0.12	27	0.5
10	1,030	7.48	70	30	92	0.24	134	30	151	107	19	0.15	27	0.5
11	930	7.47	76	26	78	0.23	122	21	129	151	18	0.09	27	0.6
12	800	7.67	34	42	74	0.23	134	30	129	68	16	0.06	24	0.4
13	726	7.38	48	22	71	0.21	110	24	107	86	15	0.09	25	0.4
14	759	7.35	30	24	94	0.21	153	15	115	38	18	0.12	26	0.4
15	768	7.69	30	25	94	0.24	122	30	107	78	14	0.12	27	0.4
16	1,236	7.99	38	29	177	0.24	122	45	151	216	8	0.18	29	0.3
17	1,575	8.08	46	35	242	0.24	92	60	235	275	10	0.15	27	0.5
18	1,353	7.97	48	29	191	0.23	61	45	160	288	11	0.09	29	0.5
19	1,720	7.60	60	35	258	0.23	122	30	204	403	11	0.09	31	0.5
20	1,257	8.15	44	13	219	0.19	110	12	160	288	17	0.12	33	0.3
21	980	7.75	28	9	179	0.15	183	30	133	104	18	0.09	25	0.2
22	1,138	7.58	36	16	186	0.20	244	60	124	96	19	0.12	28	0.3
23	905	7.73	34	17	133	0.15	153	30	107	120	18	0.06	34	0.3
24	831	7.79	30	17	127	0.12	122	30	80	154	18	0.09	36	0.3
25	990	7.65	28	16	156	0.14	165	54	98	110	13	0.09	38	0.3
26	756	8.01	26	10	124	0.11	31	66	80	139	7	0.06	36	0.3
27	940	8.08	30	14	152	0.15	92	90	107	96	19	0.12	35	0.3
28	934	8.18	30	26	133	0.14	79	57	107	154	25	0.09	30	0.3
29	818	8.03	44	20	97	0.25	122	45	89	112	19	0.06	31	0.3
30	1,207	7.74	70	31	133	0.23	214	15	129	202	38	0.09	31	0.4
31	1,142	7.93	64	30	131	0.24	244	9	133	154	40	0.09	31	0.6
32	1,225	7.92	62	37	122	0.26	244	6	173	91	50	0.12	34	0.5
33	1,070	8.40	18	16	193	0.15	31	75	89	254	28	0.06	28	0.3
34	967	8.39	22	13	191	0.13	61	45	120	192	28	0.12	26	0.3
35	903	8.10	36	14	140	0.18	61	60	89	158	25	0.09	30	0.3
36	701	8.38	20	18	113	0.16	61	45	62	113	51	0.09	30	0.3
37	623	7.97	30	16	74	0.19	92	45	71	48	27	0.12	31	0.3
38	730	8.29	42	18	87	0.19	92	45	75	86	43	0.06	34	0.3
39	721	7.98	46	13	83	0.16	122	30	71	81	37	0.12	37	0.3
40	930	7.92	42	16	124	0.17	122	30	71	149	52	0.12	36	0.3
41	780	8.07	42	19	104	0.11	61	60	57	144	32	0.09	28	0.3
42	721	8.10	42	16	94	0.10	37	48	53	154	31	0.12	27	0.3
Average	943	7.82	41	23	124	0.20	118	37	112	137	22	0.11	29	0.4

$Ca^{2+} + Mg^{2+}/HCO_3^-$ ratios around unity and low SO_4^{2-}/HCO_3^- ratios, carbonate mineral dissolution by H_2CO_3 dominates the mineral/water interaction. With increasing SO_4^{2-}/HCO_3^- equivalent ratios, the $Ca^{2+} + Mg^{2+}/HCO_3^-$ ratio also increases, and more SO_4^{2-} is needed to balance the Ca^{2+} and the Mg^{2+} in the

Table 2
Mineral saturation index of Kaboudar Ahang groundwater calculated by PHREEQUC

Wells No.	Anhydrite	Calcite	Dolomite	Gypsum	Sepiolite	Chlorite (14A)	Albite	Gibbsite	SiO_2(a)	Quartz	Alunite	$Al(OH)_3$(a)
1	−2.0	−0.6	−1.3	−1.8	−3.8	−2.0	−0.2	2.2	−0.8	0.5	−1.5	−0.5
2	−2.3	−0.7	−1.1	−2.1	−2.1	1.1	0.2	1.9	−0.7	0.6	−3.2	−0.8
3	−2.2	−0.4	−0.5	−2.0	−1.3	2.8	0.2	1.8	−0.7	0.6	−3.7	−0.9
4	−2.3	−0.4	−0.8	−2.0	−3.0	−1.1	0.1	2.0	−0.7	0.6	−2.6	−0.7
5	−2.4	−0.9	−1.8	−2.2	−2.6	0.2	0.2	2.1	−0.7	0.6	−2.8	−0.6
6	−2.0	−0.3	−0.4	−1.7	−1.6	2.7	0.5	2.2	−0.7	0.6	−2.0	−0.5
7	−2.1	−0.4	−0.9	−1.9	−3.1	−0.6	0.5	2.5	−0.6	0.6	−0.7	−0.2
8	−2.1	−0.4	−0.6	−1.8	−2.5	0.9	0.5	2.4	−0.6	0.6	−1.2	−0.3
9	−2.2	−0.2	−0.2	−2.0	−1.9	2.0	0.6	2.2	−0.6	0.6	−2.4	−0.5
10	−1.9	−0.1	−0.3	−1.6	−2.3	1.1	0.5	2.3	−0.6	0.6	−1.6	−0.4
11	−1.8	−0.2	−0.6	−1.5	−2.6	0.6	0.6	2.4	−0.6	0.6	−1.0	−0.3
12	−2.4	−0.3	−0.1	−2.2	−1.4	3.1	0.2	2.0	−0.7	0.6	−3.3	−0.7
13	−2.1	−0.5	−1.0	−1.9	−3.1	−0.8	0.3	2.3	−0.7	0.6	−1.4	−0.4
14	−2.7	−0.6	−0.8	−2.4	−3.0	−0.5	−0.1	2.3	−0.7	0.6	−1.9	−0.4
15	−2.3	−0.3	−0.4	−2.1	−1.7	2.2	0.5	2.0	−0.7	0.6	−3.2	−0.7
16	−2.0	−0.1	0.1	−1.8	−0.3	4.5	0.8	1.6	−0.6	0.7	−4.6	−1.1
17	−1.8	0.0	0.2	−1.6	0.1	5.8	1.1	1.7	−0.6	0.6	−4.4	−1.0
18	−1.8	−0.3	−0.5	−1.5	−0.6	4.4	1.0	1.8	−0.6	0.7	−3.6	−0.9
19	−1.5	−0.3	−0.4	−1.3	−1.7	2.1	1.2	2.2	−0.6	0.7	−1.3	−0.5
20	−1.8	0.1	0.1	−1.5	−0.3	4.0	1.0	1.4	−0.6	0.7	−4.5	−1.3
21	−2.2	−0.1	−0.3	−2.0	−2.2	0.2	0.4	1.6	−0.7	0.6	−4.5	−1.1
22	−2.3	−0.1	−0.2	−2.0	−2.4	0.2	0.8	2.0	−0.6	0.6	−3.0	−0.7
23	−2.2	−0.2	−0.3	−2.0	−1.5	1.8	0.8	1.8	−0.5	0.7	−3.7	−0.9
24	−2.2	−0.4	−0.6	−2.0	−1.4	1.8	0.9	1.8	−0.5	0.8	−3.9	−0.9
25	−2.3	−0.4	−0.6	−2.1	−1.9	0.7	1.1	1.9	−0.5	0.8	−3.3	−0.8
26	−2.2	−0.8	−1.7	−2.0	−0.9	2.5	0.9	1.6	−0.5	0.8	−5.3	−1.1
27	−2.3	−0.1	−0.3	−2.1	−0.4	3.8	0.9	1.5	−0.5	0.7	−6.0	−1.2
28	−2.1	−0.1	0.1	−1.9	0.4	6.0	0.6	1.4	−0.6	0.7	−6.2	−1.3
29	−2.1	0.1	0.3	−1.9	−0.3	4.4	0.5	1.5	−0.6	0.7	−5.3	−1.2
30	−1.7	0.2	0.5	−1.5	−1.2	3.0	0.9	1.9	−0.6	0.7	−2.9	−0.8
31	−1.8	0.5	1.1	−1.6	−0.3	5.1	0.9	1.9	−0.6	0.7	−3.7	−0.8
32	−2.1	0.5	1.1	−1.8	−0.1	5.5	1.0	1.9	−0.5	0.7	−4.3	−0.8
33	−2.2	−0.6	−1.0	−1.9	0.6	6.1	0.8	1.2	−0.6	0.6	−7.1	−1.5
34	−2.3	−0.3	−0.4	−2.0	0.2	5.3	0.6	1.2	−0.7	0.6	−7.2	−1.5
35	−2.1	−0.3	−1.0	−1.9	−1.3	1.9	0.8	1.5	−0.6	0.7	−5.6	−1.2
36	−2.4	−0.2	−0.2	−2.2	0.7	6.3	0.6	1.2	−0.6	0.7	−7.5	−1.5
37	−2.7	−0.3	−0.6	−2.5	−0.9	2.9	0.5	1.6	−0.6	0.7	−5.7	−1.1
38	−2.3	0.2	0.4	−2.1	0.8	6.3	0.6	1.3	−0.6	0.7	−5.2	−1.4
39	−2.1	0.1	−0.2	−1.9	−1.2	2.0	0.7	1.6	−0.5	0.8	−5.4	−1.1
40	−1.9	0.0	−0.4	−1.7	−1.5	1.2	0.8	1.6	−0.5	0.8	−4.6	−1.1
41	−2.1	−0.3	−0.4	−1.9	−0.4	4.4	0.5	1.5	−0.6	0.6	−5.7	−1.2
42	−2.0	−0.5	−0.9	−1.8	−0.4	4.2	0.4	1.5	−0.7	0.6	−5.7	−1.2

(a) Amorphous mineral.

water samples. When carbonate mineral dissolution by both H_2CO_3 and H_2SO_4 takes place and reaches equilibrium, water should have a SO_4^{2-}/HCO_3^- equivalent ratio of 0.5 and a $Ca^{2+}+Mg^{2+}/HCO_3^-$ ratio of 1.5 [22], as shown by the cross point in Fig. 3.

Stability diagram of a gibbsite, K-mica, kaolinite and K-feldspar for groundwater is shown in Fig. 4 [23]. This Figure was constructed using the log K^+/H^+ and log H_4SiO_4 activities calculated from PHREEQC. Vertical lines indicate saturation with respect to

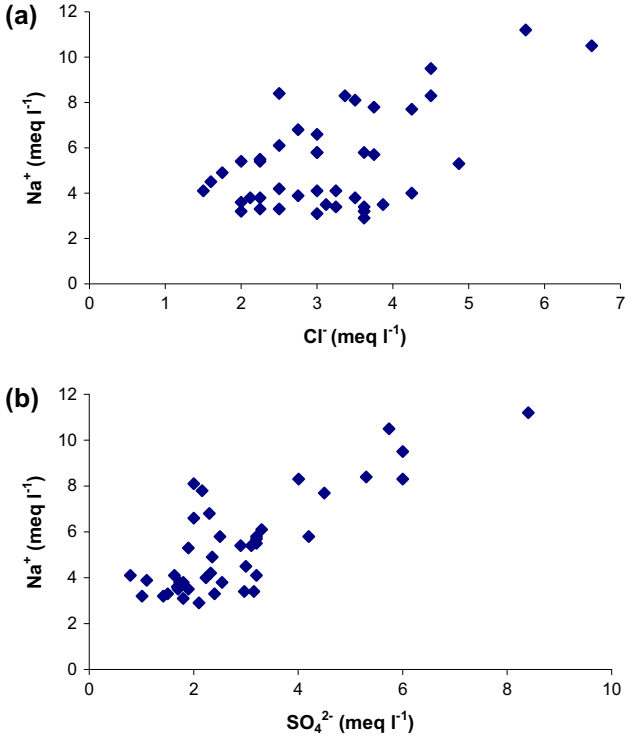

Fig. 2. Relationship between (a) Na^+ and $Cl^-$and (b) Na^+ and SO_4^{2-} Kaboudar Ahang groundwater.

Table 3
Correlation between some of the hydrochemical parameters

Variables	Correlation coefficient
Cl vs. Mg	0.59**
Cl vs. Na	0.57**
Cl vs. Ca	0.44**
HCO_3 vs. Mg	0.30*
HCO_3 vs. Na	0.01**
HCO_3 vs. Ca	0.42**
SO_4 vs. Ca	0.15
SO_4 vs. Mg	0.12
SO_4 vs. Na	0.80**
Mg vs. Ca	0.52**
SO_4 vs. Cl	0.52**
EC vs. Ca	0.36*
EC vs. Mg	0.38*
EC vs. Na	0.83**
EC vs. Cl	0.85**
EC vs. SO_4	0.80**
EC vs. HCO_3	0.26
EC vs. NO_3	−0.13

*, ** Significant at 5 and 1% level of significance, respectively.

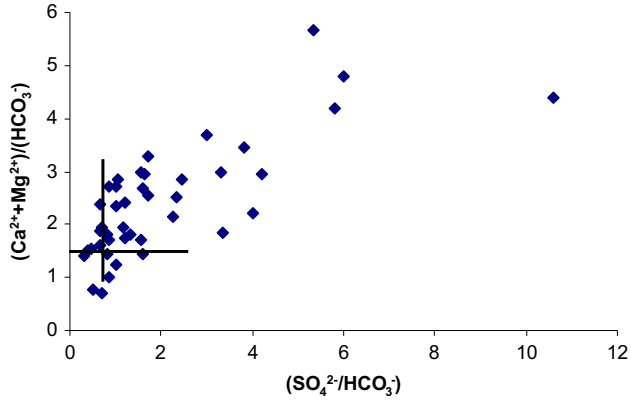

Fig. 3. Variations of $(Ca^{2+}+Mg^{2+})/(HCO_3^-)$ with (SO_4^{2-}/HCO_3^-) equivalent ratios of the Kaboudar Ahang groundwater. SO_4^{2-}/HCO_3^- equivalent ratio of 0.5 and $Ca^{2+}+Mg^{2+}/HCO_3^-$ ratio of 1.5 shown by the cross point.

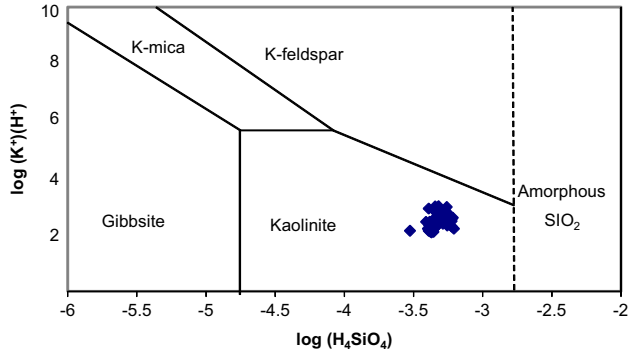

Fig. 4. Gibbsite–kaolinite–mica–potassium–feldspar–amorphous silica stability relations in aqueous solutions at 25°C and 1 atm pressure with Kaboudar Ahang data.

amorphous silica (value of log H_4SiO_4 equal to −2.7). All of the data cluster close to the kaolinite field.

4.4. Anthropogenic contamination

In arid and semi-arid regions, water resources of good quality are becoming more and more scarce and are being allocated with priority for urban water supply [24]. Salt-affected soils are commonly found in arid and semi-arid regions because of irrigation with natural saline groundwater or industrial brine discharge [25]. Anthropogenic contamination is major cause of salinization and sodification of soils and water quality degradation. Moreover, irrigation with sewage effluent from power plant located in the studied area (Fig. 1) in some parts of the studied area, which is more saline than regional groundwater increases the rate of salinization and sodification of

Table 4
Chemical composition of sewage effluent from the power plant (Jalali et al. 2008 [8])

Concentration (meq l^{-1})								EC (μS cm^{-1})	pH	SAR
Ca^{2+}	Mg^{2+}	Na^{+}	K^{+}	Cl^{-}	SO_4^{2-}	CO_3^{2-}	HCO_3^{-}			
4.3	3.8	51	0.42	21	22.2	2.7	12	6,040	7.82	25.3

groundwater and is one of the major causes of formation of saline and sodic soils in the studied area.

In some parts of studied area, sugar beet and wheat crops are being irrigated with sewage effluent due to inadequate availability of fresh surface water and ground water [8]. The sewage effluent from the power plant has a saline-sodic composition. The chemical composition of the sewage effluent from the power plant (Table 4) ([8]) indicated that Na^{+}, $Cl^{-}$and SO_4^{2-} were the most abundant cation and anions, respectively. These were followed by Ca^{2+} and HCO_3^{-} in descending order according to the concentration levels. There would be severe restrictions on use because of the high EC [26]. The incorporation of industrial and ubiquitously NaCl and other salts into aquifers will lead to the increase of Na^{+}, $Cl^{-}$and SO_4^{2-} in groundwater. The sewage effluent have a relatively low K^{+}/Na^{+} ratio, or strongly enriched in Na^{+} over K^{+}. The molar ratios of Cl^{-}/HCO_3^{-}, SO_4^{2-}/HCO_3^{-}, Na^{+}/HCO_3^{-} and K^{+}/HCO_3^{-} are 1.75, 1.85, 4.25 and 0.04, respectively. These molar ratios are very close to average molar ratios of groundwater (Cl^{-}/HCO_3^{-} = 1.63, SO_4^{2-}/HCO_3^{-}=0.74, Na^{+}/HCO_3^{-} = 2.76, K^{+}/HCO_3^{-} = 0.002). The relationship between Cl^{-}/HCO_3^{-} and SO_4^{2-}/HCO_3^{-} (Fig. 5) and Na^{+}/HCO_3^{-} and K^{+}/HCO_3^{-} (Fig. 6) in groundwater indicates that groundwater have received significant anthropogenic inputs. Thus, the use of these unsuitable waters for crop irrigation leads to their inevitable slow contamination of the soils and groundwater through the annual crop growth and evapotranspiration cycles.

Salinity and sodicity are the principal water quality concerns in irrigated areas receiving such waters [26–28]. Excessive exchangeable Na^{+}, associated with pH > 8.5, causes a degradation of the physical properties of soils, and adversely affected water and air movement, soil erodibility and plant growth [29,30]. Saline-sodic irrigation water, particularly in case of limited rainfall and high evaporation, may significantly increase soil sodicity. For instance, irrigation with saline-sodic water (EC = 300–8,500 μS cm^{-1} and SAR = 14–26 $(mmol\,l^{-1})^{1/2}$ increased soil sodicity [31].

A soil column study was conducted with two soils to assess the effects of irrigation with sewage effluent from the power plant on soil and groundwater quality [8]. The average exchangeable sodium percentage (ESP) of the soils increased during leaching from 9 to 21 and 29 to 30 after applying 5.0 and 3.5 l (about seven and six pore volumes) of sewage effluent to the soils columns, respectively. Adverse effect of high Na^{+} concentration in the wastewater on raising ESP was less pronounced in the soil having initial high ESP than in the soil with low initial ESP. Salinity of the

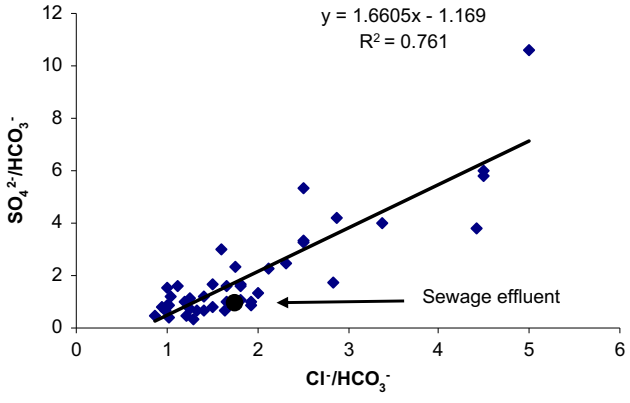

Fig. 5. Correlations of HCO_3^{-} normalized SO_4^{2-} and Cl^{-} values (molar ratios) of groundwater in Kaboudar Ahang. The molar ratio of the sewage effluent is also shown.

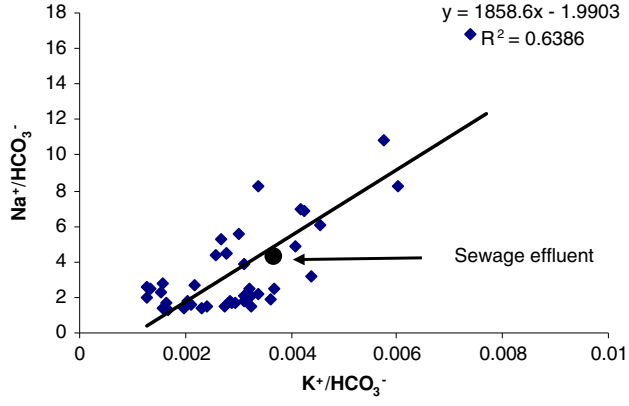

Fig. 6. Correlations of HCO_3^{-} normalized Na^{+} and K^{+} values (molar ratios) of groundwater in Kaboudar Ahang. The molar ratio of the sewage effluent is also shown.

soils was also increased with the application of sewage effluent and Mg^{2+} and K^+ were leached from the soils.

Both the sewage effluent volumes and the areas involved in wastewater irrigation are increasing as a function of time [8]. Continuous disposal of sewage effluent from power plant (which contains appreciable amounts of Na^+ ions) through irrigation in closed systems poses a serious threat of soil salinization and sodification. These problems may affect sustainability of crop production in the long run.

Variation in EC in groundwater may be related to land use and also to contamination [32,33]. Table 3 shows correlation coefficient between various anions and cations with EC. There was strong correlation between EC and Mg^{2+} ($r = 0.38$), Na^+ ($r = 0.83$), Ca^{2+} ($r = 0.36$), Cl^- ($r = 0.85$) and SO_4^{2-} ($r = 0.80$), suggesting the influence of human activities on the water chemistry or mineral dissolution.

Nitrate concentration varied from 7 to 52 mg l^{-1} with an average of 22 mg l^{-1}. The maximum safe NO_3^- concentration in drinking water was considered to be 50 mg l^{-1} (or 11.3 mg l^{-1} NO_3^-–N) according to the World Health Organization [34]. In 63% of samples, NO_3^- concentration was low (<20 mg l^{-1}) and NO_3^- concentration in 34% of samples was in the range of 20–50 mg l^{-1}. Of 42 samples, three (7%) had levels in excess of the 50 mg l^{-1} NO_3^- Nitrate is an important pollutant in environment, being generally derived from agricultural fertilizers [4], atmospheric input, human and animal excreta and bio-combustion.

To further evaluate possible hydrochemical reactions along this flowpath, inverse mass-balance models were developed using the hydrochemical reaction computer code PHREEQC [13]. Two simulations were performed. Simulation 1 describes the evolution from sample 39 to samples 28. I selected gypsum, calcite, sepiolite, dolomite, CO_2 (g) and halite as precipitating phases and albite, gibbsite, kaolinite, Ca-montmorillonite, chlorite and anhydrite as dissolving phases. Simulation 2 represents the evolution from sample 28 to sample 22 and the reacting phases were the same as in the previous model. Table 5 summarizes the species involved in phase transfers in the selected samples. All mass transfers are in mol kg^{-1}, with positive transfers indicating dissolution or ion-exchange of species from clay into groundwater.

The code found 10 models, where anhydrite dissolved in eight models, while CO_2 (g) had always precipitated, gypsum precipitated in five models, calcite, sepiolite and dolomite precipitated in 3, 2 and 1 models, respectively. Cation exchange between Ca^{2+} and Na^+ occurs with Na^+ into the solution and Ca^{2+} out of the solution. Eight models were produced for simulation 2, and are listed in Table 5. Common to all models is the precipitation of gypsum and sepiolite. Among the precipitating phases, calcite and halite precipitated in 5 and 2 models, respectively. Cation exchange between Mg^{2+} and Na^+ occurs with Na^+ into the solution and Mg^{2+} out of the solution.

A general result of all the models was the dissolution of anhydrite and precipitation of gypsum, calcite and sepiolite which justified SO_4^{2-} enrichment during the chemical evolution of groundwater. Cation exchange is also explained release of Na^+ from clay.

Table 5
Results of inverse modelling

Simulation		1	2
	Initial	39	28
	Final	28	22
Models obtained		2	24
Occurrence in models and relative mole transfer: dissolving phases	Gypsum	1 (7.6×10^{-4})	0
	CO_2 (g)	2 (5.59×10^{-4})	24 ($1.04 \times 10^{-3-5}$.18×10^{-4})
	Halite	2 (9.39×10^{-4})	12 (2.6×10^{-4})
	Sepiolite	2 (8.55×10^{-6})	12 (6.66×10^{-6})
	Dolomite	2 (2.85×10^{-3})	0
	Anydrite	1 (7.60×10^{-3})	0
	Calcite	0	14 (1.5–6.17×10^{-4})
	NaX	2 (2.55×10^{-3})	16 ($1.86 \times 10^{-3-9}$.59×10^{-4})
Occurrence in models and relative mole transfer: precipitating phases	CaX_2	2 (1.27×10^{-3})	7 (4.67–4.8×10^{-4})
	MgX_2	0	16 (4.50–4.63×10^{-4})

The amount of dissolving and precipitating is expressed as mol kg^{-1}.

5. Conclusion

The chemical composition of groundwater is dominated by Na^+, $Cl^-$and SO_4^{2-}. Based on the major constituents, in general groundwater from the studied area corresponded to NaCl and $NaSO_4$ types. Inverse geochemical modelling along flowpaths indicates the dissolution of anhydrite and precipitation of calcite, sepiolite, dolomite, gypsum and halite. The cation exchange also happens along the flow paths with Na^+ into the solution and Ca^{2+} and Mg^{2+} out of the solution along the both flow paths. Contamination of groundwater appeared to be affected by the solubility of mineral phases and discharge of sewage effluent from power plant and agricultural activities. The use of sewage effluent from power plant through irrigation in closed systems leads to their inevitable slow contamination of the soils and groundwater through the annual crop growth and evapo transpiration cycles.

References

[1] M. Jalali, Application of multivariate analysis to study water chemistry of groundwater in a semi-arid aquifer, Malayer, western Iran, Desalin. Water Treat. 19 (2010) 307–317.

[2] C.N. Rivers, K.M. Hiscock, N.A. Feast, M.H. Barrett, P.F. Dennis, Use of nitrogen isotopes to identify nitrogen contamination of the Sherwood sandstone aquifer beneath the City of Nottingham, UK, Hydrol. J 4 (1996) 90–102.

[3] A. Cardona, J.J.C. Rivera, R.H. Alvarez, E.G. Castro, Salinization in coastal aquifers of arid zones: An example from Santo Domingo, Baja California Sur, Mexico, Environ. Geol. 45 (2004) 350–366.

[4] M. Jalali, Nitrates leaching from agricultural land in Hamadan, western Iran, Agric. Ecosyst. Environ. 110 (2005) 210–218.

[5] S.C. Komor, H.W. Anderson, Nitrogen isotopes as indicators of nitrate sources in Minnesota sand-plain aquifers, Ground Water 31 (1993) 260–270.

[6] L. Wassenaar, Evaluation of the origin and fate of nitrate in the Abbotsford Aquifer using the isotopes of ^{15}N and ^{18}O in NO_3^-, Appl. Geochem. 10 (1995) 391–405.

[7] A. Umar, R. Umar, M.S. Ahmad, Hydrogeological and hydrochemical framework of regional aquifer system in Kali-Ganga sub-basin, India. Environ. Geol. 40 (2001) 602–611.

[8] M. Jalali, H. Merikhpour, M.J. Kaledhonkar, S.E.A.T.M. Van Der Zee, Effects of wastewater irrigation on soil sodicity and nutrient leaching in calcareous soils, Agric. Water Manag. 95 (2008) 143–153.

[9] A. Sepahi, Petrology of the Alvand plutonic complex with special reference on granitoids, PhD thesis, Tarbiat-Moallem University, Tehran, Iran. (in Persian), 1999.

[10] A. Baharifar, H. Moinevaziri, H. Bellon, A. Pique, The crystalline complexes of Hamadan (Sanandaj-Sirjan zone, western Iran): metasedimentary Mezoic sequences affected by Late Cretaceous tectono-metamorphic and plutonic events, C.R. Geosci. 336 (2004) 1443–1452.

[11] D.L. Rowell, Soil Science: Methods and Applications, Longman Scientific and Technical, 1994.

[12] J. Murphy, I.P. Riley, A modified single solution method for the determination of phosphate in natural waters, Anal. Chim. Acta 27 (1962) 31–36.

[13] D.L. Parkhurst, C.A.J. Appelo, PHREEQC for Windows – A Hydrogeochemical Transport Model, U.S.G.S, Denver, CO, 1999.

[14] M.T. Condesso de Melo, M.A. Marques da Silva, W.M. Edmunds, Hydrochemistry and flow modelling of the aveiro multilayer Cretaceous aquifer, Phy. Chem. Earth (B) 4 (1999) 331–336.

[15] M. Jalali, A study of the quantity/intensity relationships of potassium in some calcareous soils of Iran, J. Arid Land Res. 21 (2007) 133–141.

[16] J. Stimson, S. Frape, R. Drimmie, D. Rudolph, Isotopic and geochemical evidence of regional-scale anisotropy and interconnetivity of an alluvial fan system, Cochabamba Valey, Bolivia. Appl. Geochem. 16 (2001) 1097–1114.

[17] M.C. Hidalgo, J. Cruz-Sanjulian, Groundwater composition, hydrochemical evolution and mass transfer in a regional detrital aquifer (Baza basin, southern Spain), Appl. Geochem. 16 (2001) 745–758.

[18] A. Vengosh, R. Keren, Chemical modifications of groundwater contaminated by recharge of sewage effluent, J. Cont Hydr. 23 (1996) 347–360.

[19] A.L. Rhodes, R.M. Newton, A. Pufall, Influences of land use on water quality of diverse New England watersheds, Environ. Sci. Technol. 35 (2001) 3640–3645.

[20] K.G. Wayland, D.T. Long, D.W. Hyndman, B.C. Pijanowski, S.M. Woodhams, Sh.K. Haack, Identifying relationships between base flow geochemistry and land use with synoptic sampling and R-Mode factor analysis, J. Environ. Qual. 32 (2003) 180–190.

[21] G. Han, C_Q. Liu, Z.Q. Zhao, S. Li, G.L. Li, Water geochemistry controlled by carbonate dissolution: A study of the river waters draining karst-dominated terrain, Guizhou province, China, Chem. Geol. 204 (2004) 1–21.

[22] Y.C. Lang, C.Q. Liu, Z.Q. Zhao, S. Li, G.L. Li, Geochemistry of surface and ground water in Guiyang, China: water/rock interaction and pollution in a karst hydrological system, Appl. Geochem. 21 (2006) 887–903.

[23] S.Y. Lee, R.J. Gilkes, Groundwater geochemistry and composition of hardpans in southwestern Australian regolith, Geoderma. 126 (2005) 59–84.

[24] J.M. Beltran, Irrigation with saline water: Benefits and environmental impact, Agric. Water Manage 40 (1999) 183–194.

[25] V.P. Evangelou, M. Marsi, Influence of ionic strength on sodium–calcium exchange of two temperate climate soils, Plant Soil. 250 (2003) 307–313.

[26] R.S. Ayers and D.W. Westcott, Water quality of agriculture. FAO Irrigation and Drainage, Paper No. 29, Rome, 1985, 174 p.

[27] J.E. Ayars, K.K. Tanji, Effects of drainage on water quality in arid and semiarid lands, In: R.W. Skaggs, J. van Schilfgaarde (Eds.), Agricultural Drainage, ASA-CSSA-SSSA, Madison, WI, pp. 831–867, 1999.

[28] J.D. Oster, F.W. Schroer, Infiltration as influenced by irrigation water quality, Soil Sci. Soc. Am. J. 43 (1979) 444–447.

[29] R.K. Gupta, I.P. Abrol, Salt affected soils: Their reclamation and management for crop production, Adv. Soil Sci. 11 (1990) 223–288.

[30] S.K. Sharma, H.R. Manchanda, Influence of leaching with different amounts of water on desalinization and permeability behaviour of chloride and sulphate-dominated saline soils, Agric. Water Manag. 31 (1996) 225–235.

[31] A. Mantell, H. Frenkle, A. Meiri, Drip irrigation of cotton with saline sodic water, Irrig. Sci. 6 (1985) 95–106.

[32] M. Ellaway, B. Finlayson and J. Webb, The impact of land clearance on karst ground water: A case study from Buchan, Victoria, Australia, in: D. Drew, Hotzl (Eds.), Karst Hydrogeology and Human Activities. A.A. Balkema, Rotterdam, Netherlands, 1999, pp.66–68 .

[33] J. Gaillardet, B. Dupre, P. Louvat, C.J. Allegre, Global silicate weathering and CO_2 consumption rates deduced from the chemistry of large rivers, Chem. Geol. 159 (1999) 3–30.

[34] WHO, Guidelines for Drinking Water Quality. 1. Recommendations, second ed., World Health Organization, Geneva, 1993.